electronics

MDPI

Article

Machine-Learning-Based Validation of Microsoft Azure Kinect in Measuring Gait Profiles

Claudia Ferraris [1,*,†], Gianluca Amprimo [1,2,†], Serena Cerfoglio [3,4], Giulia Masi [2], Luca Vismara [4] and Veronica Cimolin [3,4]

[1] Institute of Electronics, Computer and Telecommunication Engineering (IEIIT), National Research Council (CNR), 10129 Turin, Italy; gianluca.amprimo@polito.it
[2] Department of Control and Computer Engineering, Politecnico di Torino, 10129 Turin, Italy; giulia.masi@polito.it
[3] Department of Electronics, Information and Bioengineering, Politecnico di Milano, 20133 Milan, Italy; serena.cerfoglio@polimi.it (S.C.); veronica.cimolin@polimi.it (V.C.)
[4] IRCCS Istituto Auxologico Italiano, Division of Neurology and Neurorehabilitation, 28824 Piancavallo, Italy; lucavisma@hotmail.com
* Correspondence: claudia.ferraris@cnr.it; Tel.: +39-011-0905404
† These authors contributed equally to this work.

Abstract: Gait is one of the most extensively studied motor tasks using motion capture systems, the gold standard for instrumental gait analysis. Various sensor-based solutions have been recently proposed to evaluate gait parameters, typically providing lower accuracy but greater flexibility. Validation procedures are crucial to assess the measurement accuracy of these solutions since residual errors may arise from environmental, methodological, or processing factors. This study aims to enhance validation by employing machine learning techniques to investigate the impact of such errors on the overall assessment of gait profiles. Two datasets of gait trials, collected from healthy and post-stroke subjects using a motion capture system and a 3D camera-based system, were considered. The estimated gait profiles include spatiotemporal, asymmetry, and body center of mass parameters to capture various normal and pathologic gait peculiarities. Machine learning models show the equivalence and the high level of agreement and concordance between the measurement systems in assessing gait profiles (accuracy: 98.7%). In addition, they demonstrate data interchangeability and integrability despite residual errors identified by traditional statistical metrics. These findings suggest that validation procedures can extend beyond strict measurement differences to comprehensively assess gait performance.

Keywords: Azure Kinect; gait analysis; validation procedure; motion capture systems; machine learning; remote monitoring; post-stroke

Citation: Ferraris, C.; Amprimo, G.; Cerfoglio, S.; Masi, G.; Vismara, L.; Cimolin, V. Machine-Learning-Based Validation of Microsoft Azure Kinect in Measuring Gait Profiles. *Electronics* **2024**, *13*, 4739. https://doi.org/10.3390/electronics13234739

Academic Editor: Michael Winter

Received: 6 November 2024
Revised: 28 November 2024
Accepted: 28 November 2024
Published: 29 November 2024

1. Introduction

Gait analysis provides valuable information for the early detection of alterations in motor control and coordination that may increase the perceived risk of falls and injuries for the individual [1,2]. Gait patterns are also extensively analyzed in clinical settings to activate targeted treatments, such as rehabilitation protocols, aimed at mitigating these risks through compensatory strategies that counteract mobility limitations associated with functional decline (e.g., in elderly individuals), chronic and progressive diseases (e.g., Parkinson's disease), or acute events (e.g., stroke) [3–7].

The instrumental and quantitative characterization of gait patterns through functional parameters enables monitoring changes over time in at-risk individuals, accelerating decision-making in response to either deterioration due to functional decline or improvements resulting from pharmacological and rehabilitation treatments [8–10]. Instrumental gait analysis is commonly performed using motion capture systems (MOCAP), the gold

standard for movement analysis in clinical settings. Although MOCAP systems provide highly accurate estimates of functional gait parameters [11–13], they are unsuitable for continuous monitoring of gait performance. Indeed, their use is generally restricted to clinical and research environments due to high costs, the need for large dedicated spaces, and the requirement for specialized technical staff [14].

In recent years, there has been growing interest in developing alternative technological solutions that are low-cost, portable, and less invasive than MOCAP systems [15,16]. These solutions employ various sensors and technologies to measure traditional gait parameters comparable to those estimated by MOCAP systems. Although these alternatives may be less accurate than gold-standard systems, they offer greater flexibility and portability. In addition, they are more suitable for frequent monitoring of gait patterns, thereby enabling earlier detection of deviations from habitual performance. The most common alternative solutions for gait analysis involve wearable sensors, such as accelerometers and inertial measurement units (IMU), and markerless camera-based approaches [17–21]. Wearable sensors are widely used to analyze human motion in various frailty conditions, including Parkinson's disease [22,23], post-stroke conditions [24,25], multiple sclerosis [26], spinocerebellar ataxia [27], and older individuals [28,29]. Similarly, camera-based approaches are effective in evaluating physiological and pathological alterations in mobility and walking patterns [30–44].

These solutions are typically validated against gold-standard MOCAP systems to demonstrate their ability to measure gait parameters accurately. This step is crucial for assessing the performance of an instrument in comparison to a reference with well-established accuracy. However, only a few of the proposed solutions have been validated against a gold standard [45–47].

Traditional validation procedures involve comparing measurements from innovative solutions, such as wearable sensors or camera-based systems, with those from a gold-standard MOCAP system, which requires placing markers on the body according to standardized biomechanical protocols. However, several factors can introduce intrinsic residual errors in the estimated gait parameters, including differences in signal processing algorithms, data sources (e.g., accelerations for wearables and movement trajectories for camera-based systems), and marker positions compared to virtual skeletal models provided by body-tracking algorithms. The question arises: Are these residual errors significant or negligible when assessing normal or pathological gait patterns? Addressing this question is crucial, especially considering that these measurement tools are not intended to replace MOCAP systems. In contrast, they are generally designed to enable rapid and widespread detection of gait alterations in settings where MOCAP systems are impractical, leaving MOCAP systems to serve as in-depth diagnostic tools in clinical settings.

Building on this foundation, this study addresses the proposed question by exploiting machine learning approaches to compare gait measurements from a traditional gold-standard system (MOCAP) with those from a 3D camera-based system using the Microsoft Azure Kinect (MAK) sensor. Through two datasets of gait trials, collected in sequence by both systems from healthy and post-stroke subjects, we aim to demonstrate that residual differences in estimated gait parameters, highlighted by traditional statistical metrics, may be irrelevant for the overall assessment of gait profiles when analyzed through an enhanced validation approach that incorporates machine learning techniques. Moreover, since the gait trials were collected sequentially by MOCAP and MAK within a short time interval, we did not expect significant differences in gait profiles due to this factor. Performance analysis of several machine learning models applied to the two datasets of gait profiles revealed consistent measurements from both systems in assessing normal and pathological gait patterns. This result was observed despite non-simultaneous data acquisition and the residual errors identified by statistical metrics, primarily caused by differences in signal sources, data processing, and parameter estimation algorithms. Consequently, the lack of data synchronization can be viewed as an added value of this study: while it might limit

the direct comparison of individual measures, it did not affect the agreement between the two systems in evaluating gait profiles.

In this field of investigation, this study offers several innovative and unique contributions. Unlike traditional validation studies, which primarily rely on statistical methods to compare gait parameters, this research integrates machine learning models into the validation process of MAK. This approach enables a comprehensive assessment of gait profiles, achieving performance comparable to the MOCAP system in evaluating normal and pathological gait profiles. Differently from other validation studies, three relevant aspects to characterizing gait profiles are combined: spatiotemporal, asymmetry, and center-of-mass parameters. In addition, this study examines the interchangeability and integrability of gait profiles captured sequentially by MOCAP and MAK systems, further demonstrating the consistency and concordance of the measurements even under more challenging conditions. Finally, by leveraging specific functions of machine learning models, this study provides insights into the features contributing to the misclassification of gait profiles. To our knowledge, no previous study has conducted such in-depth and machine-learning-based validation comparing MAK and MOCAP systems.

To conclude, this paper is organized as follows. Section 2 examines the traditional approaches for validating technology-based solutions to measure gait parameters. Section 3 outlines the methodological framework of this study. Section 4 presents the main results of the proposed machine-learning-based validation. Section 5 discusses the key findings, and Section 6 concludes with final remarks.

2. Related Works

Recent studies have explored sensor-based solutions for gait analysis, using statistical metrics to validate their performance against gold-standard systems [48].

Focusing on wearable-based solutions, Jakob et al. [49] compared a minimal set of gait parameters estimated from IMU signals using Bland–Altman plots with Limits of Agreement (LoA), Intraclass Correlation Coefficient (ICC), Spearman's correlation, and the Mann–Whitney U Test to assess measurements consistency with a marker-based gold standard system. In a similar approach, Mason et al. [17] proposed several metrics to validate their wearable-based solution, including absolute differences, Root Mean Square Error (RMSE), standard error measurement (SEM), Pearson's correlation, ICC, and Bland–Altman plots. Bland–Altman plots were also used in [50–53], often in combination with correlation metrics such as ICC [50], Lin's concordance correlation coefficient (CCC) [51], and Pearson's correlation [52]. In contrast, Desai et al. [54] employed only CCC and ICC to assess the agreement between IMUs and the reference system.

The recent review by Strongman et al. [55] identified ICC, Pearson's correlation, and Bland–Altman plots as primary metrics for validating gait measurements derived from 3D accelerations compared to the 3D marker trajectories captured by MOCAP systems. This divergence in source signals inherently requires distinct signal processing techniques and parameter estimation strategies, which may influence the final measurements.

Similar validation metrics emerge in studies involving camera-based solutions using RGB or RGB-D devices combined with markerless body-tracking frameworks. While RGB cameras are simple optical devices that capture two-dimensional color images and videos (e.g., webcams), RGB-D (or RGB-Depth) cameras are more advanced sensors that additionally provide a depth map indicating the actual distances from the camera. This information enables the 3D reconstruction of the environment, fostering more complex applications. For movement analysis, these cameras are typically paired with body-tracking algorithms capable of detecting individuals, reconstructing virtual 3D skeletal body models, and tracking real-time movements non-intrusively. In this field of investigation, Vilas-Boas et al. [34] assessed the performance of camera-based solutions on kinematic and angular parameters using Pearson's correlation, concordance correlation, and Bland–Altman plots, while Balta et al. [56] employed Mean Absolute Error (MAE), Mean Error (ME), Root Mean Square Error (RMSE), ICC, and Spearman's correlation on lower limb trajectories. Similar

metrics were also used by Liang et al. [57], Dubois et al. [35], Latorre et al. [37], and Summa et al. [58] to compare markerless and marker-based systems. Recently, Arizpe-Gómez et al. [59] validated gait parameters from the Microsoft Azure Kinect using MAE and Pearson's correlation. In contrast, Kusuda et al. [60] assessed the agreement with a MOCAP system using ICC and RMSE. For camera-based solutions, the signal sources are more homogeneous (3D marker trajectories for MOCAP systems and 2D/3D joint trajectories for markerless approaches). However, the different positioning and number of physical markers and virtual joints in skeletal models may require ad-hoc parameter estimation strategies and affect final measurements.

Limiting the comparison of measurements obtained from systems with such differing characteristics to statistical methods may be overly simplistic and reductive in motion analysis. Indeed, statistical methods aggregate data into summary metrics that can potentially obscure the intricate dynamics of complex motor patterns. Furthermore, they often rely on assumptions about data distribution that may not accurately represent movement characteristics and may be influenced by the composition and variability of the observed sample. Finally, the selection of specific metrics, tests, and statistical models can significantly influence the results, making it challenging to compare validation studies.

Given their ability to extract insights from complex datasets, machine learning models are primarily employed for regression and classification tasks. These include stratifying patient groups and clinical scores, supporting long-term patient monitoring strategies, distinguishing between physiological and pathological patterns, and tracking disease progression. However, their application in sensor validation still needs to be improved [48]. In this context, the present study investigates the feasibility of using machine learning approaches to enhance the validation of gait measurement solutions and address this gap. Specifically, it examines how machine-learning models could complement traditional statistical analyses by evaluating the significance of residual differences in assessing normal and pathological gait profiles. Machine learning approaches offer significant advantages. Unlike statistical methods, they can identify complex dependencies and dynamics within the data, capturing nuanced movement profiles that might otherwise be overlooked. In addition, they can exploit multiple features together, allowing for a more comprehensive assessment of movement patterns than single aggregate measures. Finally, these models can provide interpretable comparisons and valuable insights, enriching the validation process. These peculiarities could extend the use of machine learning to enhance current validation strategies, especially when comparing systems that exhibit substantial technological and methodological differences.

3. Materials and Methods

3.1. Data Collection

The datasets used in this study derive from walking data previously collected during the REHOME project [61]. Gait trials were conducted on a 10-m walkway in a hospital laboratory and recorded using a standard marker-based MOCAP system (VICON, Oxford Metrics Ltd., Oxford, UK) and a markerless solution based on the MAK sensor (Microsoft Inc., Redmond, WA, USA), as described in some recent studies [43,44,62]. Although simultaneous acquisition is typical in validation studies, the gait trials were collected sequentially to avoid potential interference between systems that rely on infrared technologies. Each subject was recorded separately by MOCAP and MAK systems, with no overlap. This approach was selected to demonstrate that the Azure Kinect can still provide gait profiles consistent with those obtained by MOCAP. Therefore, the lack of synchronization can be considered an additional positive factor in further validating the agreement between the two systems. Furthermore, given the short duration of each gait trial, we did not expect significant variations in gait patterns due to non-simultaneous acquisitions.

For three-dimensional instrumental gait analysis with the MOCAP system, a configuration of 27 spherical retro-reflective markers (size: 15 mm) was applied to each participant's body, following the modified Plug-In Gait model [63,64] (Figure 1a). In contrast, the MAK

sensor provides a body-tracking algorithm that estimates a 3D skeletal model consisting of 32 virtual joints, which approximate specific anatomical reference points [65], thus mapping human body movements in real-time. Since certain joints were not relevant to this study (e.g., those of the face and hands), only 20 virtual joints from the MAK skeletal model were considered (Figure 1b). The body-tracking algorithm and the device management libraries, installed through the available SDKs, worked on a mini-PC with hardware specifications satisfying the requirements for real-time performance. Therefore, body detection and tracking were managed locally, with no data transfer to cloud platforms, thus avoiding privacy and data security concerns.

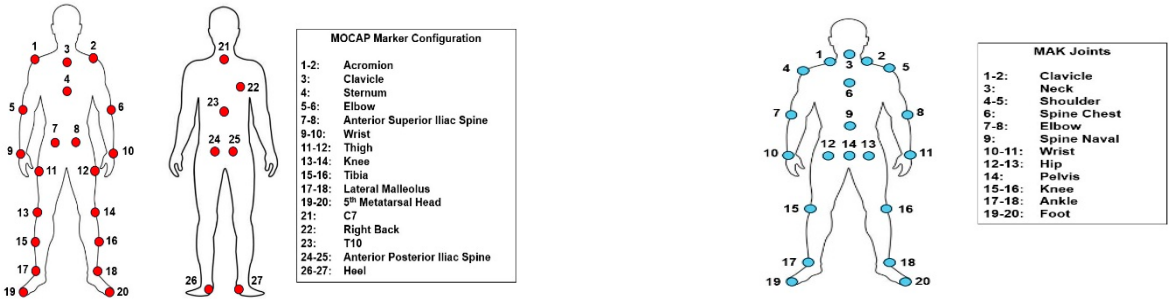

Figure 1. (**a**) MOCAP marker configuration (27 markers) placed on the front and back of the body. (**b**) MAK skeletal model (20 virtual joints) tracked on the frontal side of the body.

To comprehensively explore the measurement performance of the MAK system in comparison with MOCAP, two groups of adult volunteers (aged $\geq$ 18 years) were involved: healthy controls (HC) and post-stroke subjects (PS). Specifically, the HC group consisted of 42 subjects (45% male, 55% female) with no history of injury in the previous year and no musculoskeletal or neurological disorders affecting their walking ability. The PS group included 35 subjects (55% male, 45% female) with unilateral hemiplegia (bilateral disability was an exclusion criterion) who were able to walk 10 m without assistance. Statistical differences in the composition of the two groups were irrelevant to the analysis, as the primary objective was to compare the MOCAP and MAK systems in measuring gait patterns independent of gender, height, weight, age, and physical condition. Each participant performed the gait trials under the supervision of technical and clinical professionals after a preliminary familiarization with the instrumentation and protocol instructions. Two datasets of gait profiles were then created: one for MOCAP (DB_MOCAP) and one for MAK (DB_MAK), each containing 42 gait profiles from healthy controls and 35 gait profiles from post-stroke subjects.

3.2. Signal Processing and Gait Parameters Estimation

The two datasets consist of unique gait profiles obtained from gait trials collected using MOCAP and MAK systems. While both systems recorded three-dimensional trajectories for each gait trial related to physical markers and virtual joints, respectively, they operated at different sampling rates: MOCAP at 100 Hz and MAK at 30 Hz. More importantly, the physical markers (MOCAP) and virtual joints (MAK) differed in their body positions, as shown in Figure 1a,b. These factors, combined with the non-simultaneous acquisitions, ultimately affect the algorithms used to estimate gait parameters and may result in measurement discrepancies.

Furthermore, to make the analysis of gait more comprehensive, this study incorporated three categories of parameters to create gait profiles: spatiotemporal parameters, body center of mass (BCOM) parameters, and asymmetry parameters. The inclusion of BCOM and asymmetry parameters aimed to capture abnormal body sways and gait laterality, which are particularly prevalent in pathological populations. The resulting set of

estimated gait parameters formed the unique gait profile (UGP) consisting of 18 features that summarize each participant's gait trial, as illustrated in Figure 2.

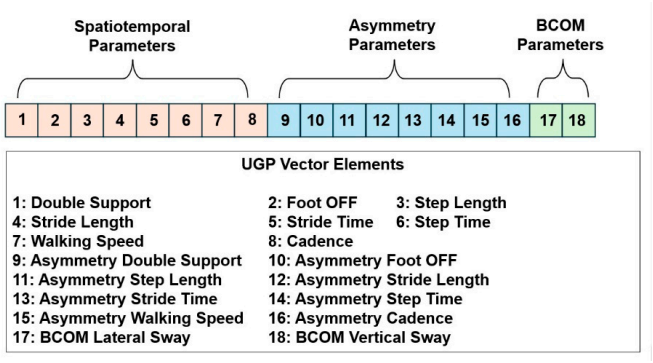

Figure 2. Structure of the Unique Gait Profile vector, including spatiotemporal parameters, asymmetry parameters, and BCOM parameters.

For the MOCAP system, the spatiotemporal gait parameters were automatically computed using Nexus (Version 1.8, VICON, Oxford Metrics Ltd., Oxford, UK) and Polygon (Version 2.4, VICON, Oxford Metrics Ltd., Oxford, UK), which are standard software for tracking and analyzing MOCAP raw data. This processing followed the manual definition of gait events (specifically, right/left heel strike and toe-off) for steps performed near the laboratory's force plates [43,44]. Spatiotemporal parameters were estimated separately for the left and right sides of the body and then averaged to be assembled into the UGP alongside BCOM and asymmetry parameters. The BCOM position was automatically calculated as the midpoint of the vector connecting the Anterior Superior Iliac Spine (ASIS) markers to the Posterior Superior Iliac Spine (PSIS) markers.

For the MAK system, spatiotemporal parameters were estimated from ankle trajectories, as these joints provide more accuracy and robustness compared to the feet [66,67]. Initial data preprocessing was performed in MATLAB© (2024a version) and included a resampling procedure at 50 Hz to reduce jitter effects during acquisition and improve spatial resolution. This was followed by low-pass filtering to attenuate high-frequency noise. Then, a step segmentation procedure based on the depth component (i.e., the distance from the MAK) of the left and right ankle joints was applied, enabling the extraction of both primary and derived spatiotemporal parameters. The step segmentation procedure involved identifying stationary periods (stance phases) and in-motion periods (swing phases), as described by Ferraris et al. and Cimolin et al. [43,44]. From the alternation of these periods, the same spatiotemporal parameters and features were computed for the MOCAP system. Unlike MOCAP, the BCOM position for MAK was estimated as the midpoint of the vector connecting the hip joints.

Lateral and vertical BCOM sways within gait cycles were calculated to detect potential abnormal imbalances during walking, which are common in individuals with pathological gait patterns. Gait laterality information was preserved through the asymmetry parameters, which were computed for all spatiotemporal parameters in both MOCAP and MAK, as indicated by Equation (1) [68]:

$$ASYM_P = |P_{LEFT} - P_{RIGHT}| / (0.5 * (P_{LEFT} + P_{RIGHT})) * 100\%, \quad (1)$$

In the equation above, P represents one of the spatiotemporal parameters listed in Table 1, with P_{LEFT} and P_{RIGHT} denoting the values estimated for the left and right sides, respectively.

Since multiple gait cycles can be identified within the gait analysis area, the spatiotemporal and BCOM parameters were averaged across all detected gait cycles. In contrast, the asymmetry parameters were calculated using the final values obtained for the left and right

sides. Table 1 provides a detailed list of the gait parameters that form the UGP, along with their definitions and units.

Table 1. List of gait parameters and categories included in the Unique Gait Profile (UGP).

Category	Parameter	Full Name	Meaning	Unit
SPATIO TEMPORAL	DS	Double Support	Time steady with both feet	s
	FOFF	Foot OFF	Stance phase (% of gait cycle)	%
	STEPL	Step Length	Length of one-foot step	m
	STRIDEL	Stride Length	Length of a complete gait cycle	m
	STRIDET	Stride Time	Duration of a complete gait cycle	s
	STEPT	Step Time	Duration of one-foot step	s
	WSPEED	Walking Speed	Ratio between stride length and stride time	m/s
	CAD	Cadence	Number of steps in a time unit	step/min
ASYMMETRY	$ASYM_{DS}$	Double Support asymmetry	Asymmetry between left and right double support	%
	$ASYM_{FOFF}$	Foot OFF asymmetry	Asymmetry between left and right stance phases	%
	$ASYM_{STEPL}$	Step Length asymmetry	Asymmetry between left and right step length	%
	$ASYM_{STRIDEL}$	Stride Length asymmetry	Asymmetry between left and right stride length	%
	$ASYM_{STRIDET}$	Stride Time asymmetry	Asymmetry between left and right stride time	%
	$ASYM_{STEPT}$	Step Time asymmetry	Asymmetry between left and right step time	%
	$ASYM_{WSPEED}$	Walking Speed asymmetry	Asymmetry between left and right walking speed	%
	$ASYM_{CAD}$	Cadence asymmetry	Asymmetry between left and right cadence	%
CENTER OF MASS	$BCOM_{ML}$	BCOM Lateral Sway	Left-right BCOM sways within gait cycles	mm
	$BCOM_{V}$	BCOM Vertical Sway	Up-down BCOM sways within gait cycles	mm

3.3. MOCAP vs. MAK Systems: Traditional Validation Methods

This analysis aims to highlight the similarities and differences between the two systems using the DB_MOCAP and DB_MAK datasets. It includes traditional validation metrics and methods, treating the gait profiles of healthy controls and post-stroke individuals as simple measurements without accounting for their normal or pathological origins. All data analyses were performed using custom MATLAB© (version 2024a) scripts.

Firstly, the Kolmogorov–Smirnov test was applied to all parameters from both datasets to assess the consistency of their data distributions and determine the suitability of parametric or non-parametric statistical tests. As the normality test revealed non-normal distributions for all parameters (see Section 4.1), non-parametric tests and metrics were selected for subsequent analysis phases.

Specifically, the Mann–Whitney U test for independent samples was employed to identify statistical differences between the parameters obtained from MOCAP and MAK, treating them as independent measurement systems. In addition, the Mean Absolute Error (MAE) and Root Mean Square Error (RMSE) were calculated to evaluate the accuracy of the parameter estimates for both systems.

In parallel, Spearman's correlation coefficient was applied to explore the relationship between MOCAP and MAK parameters. This same coefficient was also used to examine the correlation between each parameter and the participant groups, where the '1' label was assigned to healthy control gait profiles and the '0' label to post-stroke gait profiles.

Finally, the Intraclass Correlation Coefficient (ICC) for absolute agreement and the Concordance Correlation Coefficient (CCC) was used to assess the consistency, reliability, and concordance between the measurements from the two systems. As discussed in Section 2, these statistical metrics align with the standard statistical approaches commonly used for validating the performance of two measurement systems.

3.4. MOCAP vs. MAK Systems: Enhanced Validation by Machine Learning

This analysis aims to demonstrate that, although traditional validation metrics reveal differences in measuring gait parameters, these discrepancies do not influence the overall assessment of normal or pathological gait performance. A machine learning approach using supervised classifiers was employed to support this hypothesis. The gait profiles of healthy controls and post-stroke individuals from the DB_MOCAP and DB_MAK datasets were analyzed separately, with labels assigned to each unique gait profile (UGP): '1' for healthy controls (42 UGPs) and '0' for post-stroke individuals (35 UGPs).

The analysis was structured into three phases, as illustrated in Figure 3.

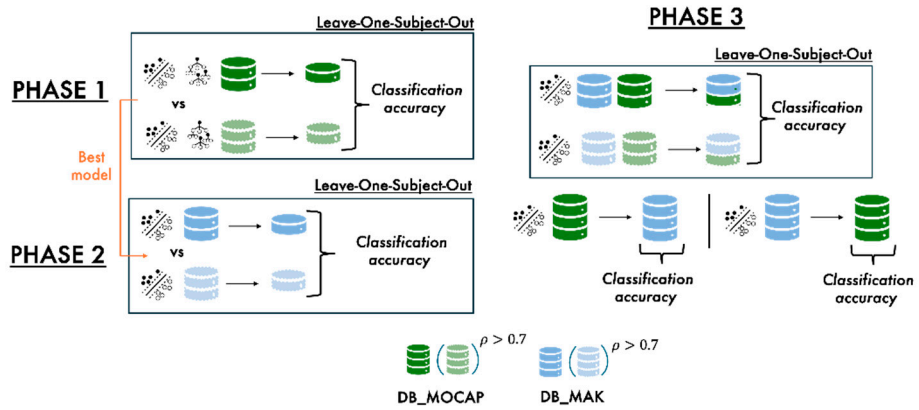

Figure 3. Summary of the 3-step enhanced validation protocol through machine learning.

In the first phase, various supervised classifiers were applied to the DB_MOCAP dataset to identify the best model for distinguishing healthy control UGPs from post-stroke UGPs. The UGPs in the DB_MOCAP were used as input to train the classifiers, using the Leave-One-Out method for cross-validation. Two conditions were considered for training: using the entire UGP (i.e., all parameters) or a subset of more significant parameters, specifically those with an absolute value of Spearman's correlation coefficient between MOCAP and MAK greater than 0.7.

The following models, available in MATLAB Classification Learner Toolbox, were considered in the first phase:

- Fine Tree: A decision tree model that splits the data into smaller subsets to maximize separation between different classes, resulting in a deep tree structure where each split corresponds to a dataset feature. The depth and granularity of the splits enable the model to capture fine-grained patterns in the data.
- Linear Discriminant Analysis (LDA): A model that identifies a linear combination of features that best separates two or more classes, using a decision boundary that maximizes the separation between the classes while minimizing the variance within each class.
- Naive Bayes (NB): A model that assumes the dataset features (or predictors) are independent, given the class label. It estimates the likelihood of each feature for each class and combines these probabilities with the prior probability of each class to make predictions.
- Support Vector Machine (SVM): A model that finds the optimal decision boundary (hyperplane) to best separate different classes in a dataset by maximizing the margin between them. The margin is the distance between the closest data points (support vectors) of different classes and the decision boundary, which enhances the model's generalization ability. SVMs can operate with linear (a straight hyperplane to separate the classes) or non-linear kernels (transforming the data into a higher-dimensional space where linear separation becomes possible).
- K-Nearest Neighbors (KNN): A model that classifies a data point based on the majority class of its nearest neighbors in the feature space. The 'K' represents the number of

neighbors from the training dataset considered to make the classification decision, determined by the distance between the data points and other points in the training set.

- Boosted Trees (BOOST Tree): An ensemble learning method that combines the predictions of multiple decision trees to improve classification accuracy through a more robust model. In practice, multiple weak learners (typically shallow decision trees) are combined into strong learners. Each tree in the sequence is trained to correct the errors of its predecessors, thereby improving the overall model's performance.

In the second phase, the best model identified from the DB_MOCAP dataset was applied to the DB_MAK dataset to compare performance and determine whether UGPs derived from MAK data can be evaluated similarly to those from MOCAP data. Estimating the posterior probabilities associated with each observation (UGP) from the two groups (HC and PS) provided in-depth insight into the predictive capabilities of the trained models. This procedure helped explain the origins of any misclassifications.

In the third phase, the performance of the best model trained on DB_MOCAP was evaluated using DB_MAK as a testing set, and vice versa—i.e., the best model trained on DB_MAK was evaluated using DB_MOCAP as a testing set—to verify their interchangeability, which is possible only if the measurements are similar and consistent. Following this, the DB_MOCAP and DB_MAK datasets were combined into a new, double-sized dataset to assess their integrability without compromising overall prediction performance.

4. Results

4.1. MOCAP vs. MAK Systems: Validation Using Statistical Methods

The Kolmogorov–Smirnov test indicated a non-normal distribution for all parameters in both datasets, emphasizing the similarity and consistency of the measurements from both systems. Table 2 presents the parameter values as medians and interquartile ranges (first and third quartiles) according to non-parametric statistics. In addition, Spearman's correlation coefficients (ρ_0 indicating the correlation between MOCAP and MAK; ρ_1 indicating the correlation within participant groups for MOCAP and MAK), along with MAE, RMSE, ICC, and CCC, are reported to further support the evidence of measurement consistency (Table 3).

Table 2. Median with first and third quartiles for all parameters.

Parameter	MOCAP Median [1st–3rd Quartiles]	MAK Median [1st–3rd Quartiles]
DS	0.233 [0.179–0.402]	0.270 [0.194–0.493]
FOFF	61.059 [59.285–64.692]	61.967 [59.507–68.524]
STEPL	0.612 [0.386–0.698]	0.604 [0.390–0.706]
STRIDEL	1.241 [0.766–1.399]	1.148 [0.757–1.371]
STRIDET	1.107 [1.023–1.462]	1.120 [1.050–1.460]
STEPT	0.548 [0.505–0.740]	0.560 [0.525–0.721]
WSPEED	1.107 [0.571–1.394]	1.043 [0.607–1.262]
CAD	108.449 [82.157–117.290]	107.151 [82.218–114.317]
$ASYM_{DS}$	5.479 [2.565–10.534]	5.128 [1.512–12.871]
$ASYM_{FOFF}$	4.958 [2.067–10.775]	2.358 [1.311–4.994] *
$ASYM_{STEPL}$	6.557 [2.352–11.925]	5.975 [2.459–13.804]
$ASYM_{STRIDEL}$	1.670 [0.596–3.288]	2.420 [1.162–4.321] *
$ASYM_{STRIDET}$	2.522 [1.359–3.908]	0.987 [0.338–2.430] *
$ASYM_{STEPT}$	6.360 [1.730–15.437]	4.959 [1.971–13.533]
$ASYM_{WSPEED}$	2.323 [1.203–3.813]	2.223 [1.012–3.738]
$ASYM_{CAD}$	2.522 [1.359–3.908]	0.987 [0.338–2.43] *
$BCOM_{ML}$	50.378 [38.031–87.047]	49.179 [42.281–66.122]
$BCOM_{V}$	38.808 [24.219–48.124]	34.414 [29.222–43.989]

* The symbol indicates parameters with significant statistical differences ($p < 0.05$) between MOCAP and MAK, according to the Mann–Whitney U Test.

Table 3. Correlation, errors, agreement, and concordance metrics between MOCAP and MAK.

Parameter	ρ_0 (MOCAP vs. MAK)	ρ_1 (MOCAP vs. Groups)	ρ_1 (MAK vs. Groups)	MAE	RMSE	ICC	CCC [Range]
DS	0.979 *	−0.663 *	−0.685 *	0.052	0.070	0.976 *	0.976 [0.962–0.985]
FOFF	0.892 *	−0.685 *	−0.781 *	2.126	3.234	0.861 *	0.861 [0.795–0.907]
STEPL	0.982 *	0.867 *	0.859 *	0.026	0.035	0.982 *	0.982 [0.971–0.988]
STRIDEL	0.983 *	0.869 *	0.846 *	0.053	0.075	0.978 *	0.978 [0.967–0.986]
STRIDET	0.988 *	−0.707 *	−0.704 *	0.050	0.074	0.983 *	0.983 [0.975–0.988]
STEPT	0.983 *	−0.723 *	−0.675 *	0.033	0.041	0.980 *	0.980 [0.969–0.987]
WSPEED	0.982 *	0.889 *	0.873 *	0.073	0.113	0.970 *	0.970 [0.955–0.980]
CAD	0.981 *	0.801 *	0.775 *	3.875	5.470	0.972 *	0.972 [0.958–0.981]
$ASYM_{DS}$	−0.015	0.223	0.347	8.652	12.034	−0.015	−0.014 [−0.213–0.187]
$ASYM_{FOFF}$	0.462	−0.588 *	−0.333	5.831	9.100	0.172	0.246 [0.132–0.353]
$ASYM_{STEPL}$	0.820 *	−0.374 *	−0.438 *	7.528	12.123	0.799 *	0.796 [0.707–0.861]
$ASYM_{STRIDEL}$	0.117	−0.215	−0.031	2.201	2.907	0.072	0.104 [−0.097–0.296]
$ASYM_{STRIDET}$	0.073	0.004	0.125	2.229	2.834	−0.038	0.058 [−0.120–0.233]
$ASYM_{STEPT}$	0.840 *	−0.606 *	−0.581 *	6.736	10.329	0.728 *	0.729 [0.640–0.800]
$ASYM_{WSPEED}$	0.055	−0.350	0.070	2.404	3.272	0.061	0.055 [−0.170–0.273]
$ASYM_{CAD}$	0.073	0.004	0.125	2.229	2.834	−0.038	0.058 [−0.120–0.233]
$BCOM_{ML}$	0.882 *	−0.792 *	−0.647 *	14.160	17.914	0.792 *	0.791 [0.721–0.846]
$BCOM_{V}$	0.787 *	0.573 *	0.237	7.289	8.878	0.777 *	0.774 [0.671–0.848]

* The symbol indicates parameters with significant Spearman's correlation ($p < 0.05$) and significant ICC agreement ($p < 0.05$) between the systems.

As expected, Table 2 highlights deviations in all measurements, although significant differences are observed only for four asymmetry parameters. This outcome is not unusual, as asymmetry parameters are derived from primary spatiotemporal measurements, and thus, they can be influenced by the propagation of measurement errors for the reasons previously mentioned. Furthermore, while spatiotemporal parameters, such as step length and step time, generally exhibit consistent distributions across multiple trials, slight variations may occur in other parameters due to natural fluctuations in motor control. These fluctuations are more evident in subtle gait cycle variables and derived parameters, such as asymmetry measures. This phenomenon is observable not only in pathological subjects but also in healthy controls [69,70]. Nevertheless, the results suggest that the MAK system can effectively measure all the gait parameters considered, showing good agreement with those measured by MOCAP despite differences in biomechanical models, parameter estimation algorithms, and the expected slight variations in gait patterns during subsequent recordings.

These considerations are further supported by the results presented in Table 3. Regarding the ICC, almost all spatiotemporal parameters, except for the FOFF parameter, show correlation values greater than 0.9, indicating excellent agreement between the two systems. A good agreement is observed regarding the FOFF and BCOM parameters, with values ranging from 0.75 to 0.9. In contrast, asymmetry parameters show the weakest results: only $ASYM_{STEPL}$ and $ASYM_{STEPT}$ exhibit good agreement, while the others show unrelated values. This trend is consistent with the results for CCC and Spearman's correlation coefficient (ρ_0). Both MOCAP and MAK demonstrate similar outcomes in terms of the correlation between parameters and participant groups, with the magnitude and direction of the monotonic relationship aligning for significant parameters. The correlation values range from moderate ($|\rho_1| > 0.3$) to very strong ($|\rho_1| > 0.7$) for both MOCAP and MAK.

These findings suggest strong agreement and consistency between the two systems in measuring gait parameters, with particularly robust relationships for spatiotemporal and BCOM parameters. In contrast, the relationship for asymmetry parameters is weaker. However, it is important to emphasize that asymmetry parameters are more informative when assessing post-stroke gait profiles, as healthy controls typically do not exhibit laterality. This factor may have influenced the overall results of the asymmetry correlations.

4.2. MOCAP vs. MAK Systems: Validation Using Machine Learning

In the first phase, the DB_MOCAP dataset was used as input for the supervised classifiers, considering both the entire UGP (i.e., all gait parameters) and a subset of 12 gait parameters with significant correlation ($|\rho_0| > 0.7$) as shown in Table 3. Accuracy was used as the metric to evaluate model performance, along with the number of errors in assessing healthy control (HC) and post-stroke (PS) UGPs. The results are presented in Table 4.

Table 4. Models' accuracy and number of errors using DB_MOCAP.

	All Parameters			12 Parameters		
Model	**Accuracy (%)**	**# Errors (HC Group)**	**# Errors (PS Group)**	**Accuracy (%)**	**# Errors (HC Group)**	**# Errors (PS Group)**
Fine Tree	97.4%	0	2	97.4%	0	2
LDA	97.4%	0	2	97.4%	0	2
NB	97.4%	0	2	97.4%	0	2
SVM (Linear)	**98.7%**	0	1	**98.7%**	0	1
SVM (Quadratic)	96.1%	0	3	96.1%	0	3
KNN (K = 3)	96.1%	0	3	97.4%	0	2
BOOST Tree	97.4%	0	2	94.8%	2	2

The results indicate that the SVM model with a linear kernel is the most effective for accurately assessing the gait profiles of healthy controls and post-stroke individuals using the DB_MOCAP dataset as input. The optimality of the linear kernel suggests that gait profiles are inherently separable by a linear boundary (hyperplane) in their original mathematical space. This separability may be partially lost when they are reprojected into a higher-dimensional space (quadratic kernel). As a secondary benefit, computations with the linear kernel are more efficient than with a quadratic kernel due to its lower complexity. Moreover, the model performance remains consistent even when the parameter set is reduced to those showing the strongest correlations ($|\rho_0|$) between MOCAP and MAK. Other models also maintain consistent performance after reducing the parameter set, except for KNN, which shows improved accuracy, and BOOST Tree, which shows a decline in performance. Notably, errors predominantly occur in post-stroke UGPs, with a minimum of one and a maximum of three errors, suggesting that some gait profiles of post-stroke individuals were misclassified as healthy controls. However, this is consistent with the fact that PS UGPs represent post-stroke individuals with varying degrees of disability and levels of functional recovery.

In the second phase of the analysis, the SVM model with a linear kernel was trained on the DB_MAK dataset. The results are presented in Table 5. In addition to the number of classification errors for the HC and PS groups, the specific indexes (IDs) of the misclassified records are provided for further comparison.

Table 5. Accuracy of SVM models, errors, and misclassification IDs for HC and PS groups.

	All Parameters			12 Parameters		
Dataset	**Accuracy (%)**	**# Errors (HC Group)**	**# Errors (PS Group)**	**Accuracy (%)**	**# Errors (HC Group)**	**# Errors (PS Group)**
DB_MOCAP	98.7%	0	1 (ID: 64)	98.7%	0	1 (ID: 64)
DB_MAK	98.7%	0	1 (ID: 64)	98.7%	0	1 (ID: 64)

The results indicate that the SVM models achieved identical performance when trained on DB_MAK and DB_MOCAP datasets, confirming that the differences in the estimated parameters from the MAK system do not affect the assessment of the overall gait profiles of healthy controls and post-stroke individuals. Moreover, the accuracy is high, with only a single misclassification involving the same post-stroke individual (ID 64) in both datasets.

Furthermore, applying the MATLAB '*fitPosterior*' function to the SVM-trained model allows one to determine the posterior probabilities for each observation, providing deeper insights into the model's predictions and enhancing the interpretability of its outcomes. Based on the Platt scaling procedure [71], the model's decision scores are converted into probabilistic values, helping to understand the confidence in correct predictions and identify the sources of misclassifications. This analysis also enables the assessment of the overall probability of correctly predicting observations from both the HC and PS groups, considering the trained models in both conditions (using all UGP parameters and only a subset). The results of this analysis are presented in Table 6.

Table 6. Prediction performance of trained models (average probability and standard deviation) for HC and PS groups.

	All Parameters		**12 Parameters**	
Dataset	**HC Probability**	**PS Probability**	**HC Probability**	**PS Probability**
DB_MOCAP	0.974 ± 0.07	0.966 ± 0.16	0.986 ± 0.03	0.963 ± 0.17
DB_MAK	0.970 ± 0.07	0.964 ± 0.16	0.952 ± 0.08	0.946 ± 0.17

The results indicate that the trained SVM models exhibit similar probabilities in correctly predicting healthy control and post-stroke observations, especially when using all the UGP parameters. The probability is higher for the HC group (42 UGPs), with a small standard deviation, while performance slightly decreases for the PS group (35 UGPs). When using a subset of parameters (12-parameter condition), the SVM models show different trends for the HC group, with an improvement in probability for DB_MOCAP and a decline for DB_MAK. Conversely, performance decreases for the PS group across both datasets. However, it is important to note that the results for the PS group also include the probability associated with the misclassified observation (ID 64). A detailed exploration of the prediction probabilities for this UGP reveals that it was predicted as a healthy control with a probability of 0.945 (only 0.055 as post-stroke) for DB_MOCAP and 0.978 (only 0.022 as post-stroke) for DB_MAK. This element has obviously contributed to a reduction in the overall model's prediction accuracy for the PS group. After excluding this misclassified observation, the mean probabilities and standard deviations for the PS group improved, as shown in Table 7.

Table 7. Prediction performance of trained models (average probability and standard deviation) for HC and PS groups without ID 64.

	All Parameters		**12 Parameters**	
Dataset	**HC Probability**	**PS Probability**	**HC Probability**	**PS Probability**
DB_MOCAP	0.974 ± 0.07	0.993 ± 0.02	0.986 ± 0.03	0.991 ± 0.04
DB_MAK	0.970 ± 0.07	0.991 ± 0.02	0.952 ± 0.08	0.972 ± 0.07

Moreover, the analysis of the prediction probability associated with the misclassified observation (ID 64) suggests that its UGP may be more similar to those of healthy individuals than post-stroke individuals. A closer examination of the UGP parameters supports this hypothesis. Figure 4 displays the UGP parameters of the misclassified observation (black circles) in comparison to the UGP parameters of the HC group (light blue circles) and the PS group (red circles).

When compared to HC and PS groups, the position of UGP parameters (ID 64) reveals that the subject's gait performance aligns more closely with healthy patterns than with post-stroke patterns. All spatiotemporal parameters, as well as BCOM parameters, fall within the region associated with the HC group. This trend is also observed in some

asymmetry parameters, except for $ASYM_{CAD}$ and $ASYM_{WSPEED}$, which, however, were less relevant for the model's prediction ($|\rho_0| < 0.1$).

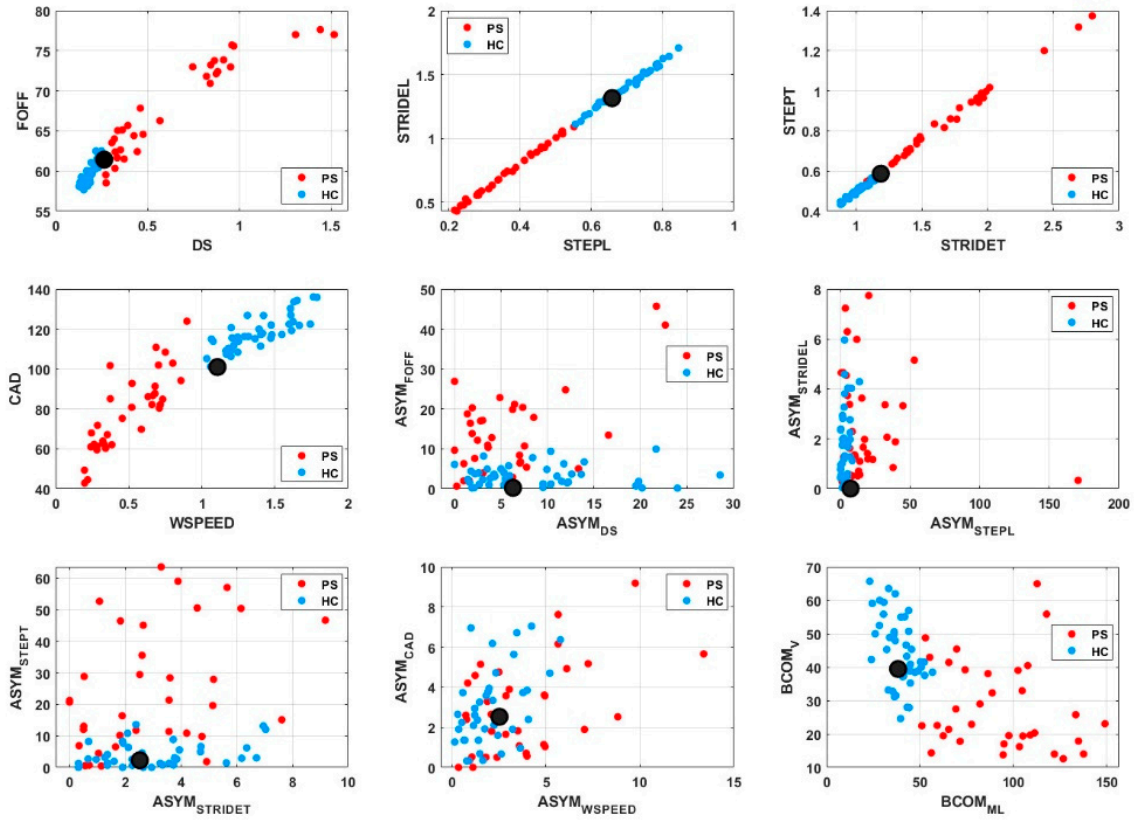

Figure 4. Position of the UGP parameters (black dots) related to the misclassification (ID 64) compared to the HC and PS groups.

The final phase evaluated the cross-prediction capabilities of the two datasets to complete the performance analysis of MOCAP and MAK data using machine learning. The performance of the SVM model trained on DB_MOCAP (using all UGP parameters) was assessed by testing it on DB_MAK to evaluate how well the MOCAP dataset generalizes to MAK data. Similarly, the performance of the SVM model trained on DB_MAK was evaluated by testing it on DB_MOCAP for the same purpose. Finally, the two datasets were merged, and the prediction capabilities were evaluated on this new combined dataset, as in data augmentation approaches. The results are presented in Table 8.

Table 8. Accuracy of the SVM linear models in the cross-prediction phase.

Cross-Prediction Case	Accuracy (%)	# Errors HC Group	# Errors PS Group
SVM Training on DB_MOCAP; Testing on DB_MAK	97.4%	0	2 (ID: 61, 64)
SVM Training on DB_MAK; Testing on DB_MOCAP	96.1%	1 (ID: 6)	2 (ID: 61, 64)
SVM Training and Validation on DB_MOCAP and DB_MAK merge dataset	98.7%	0	2 (ID: 64, 141)

This analysis leads to several specific considerations. In the first case (SVM trained on DB_MOCAP and tested on DB_MAK), a new misclassification of a post-stroke subject (ID 61) was identified, in addition to ID 64. Despite the differences in measurements, the SVM model trained on MOCAP data still effectively predicts gait profiles from MAK data.

In the second case (SVM trained on DB_MAK and tested on DB_MOCAP), a new misclassification was observed in the healthy group (ID 6). This misclassification likely

involves a healthy subject positioned near the decision boundaries created by the SVM model trained on DB_MAK. As for post-stroke subject ID 64, who exhibits a profile similar to the HC group, the misclassified healthy subject (ID 6) might have a gait profile closer to the PS group for specific UGP parameters. Nevertheless, despite measurement differences, the SVM model trained on MAK data continues to predict nearly all gait profiles from the MOCAP data accurately.

Finally, in the third case, the SVM model trained on the combined dataset (i.e., 84 UGPs for healthy controls and 70 UGPs for the PS group) achieved the same accuracy as when trained on the individual datasets (see Table 5). The two misclassifications (ID 64 and ID 141) correspond to the same post-stroke subject measured with MOCAP (ID 64) and MAK (ID 141). This result suggests that merging the two datasets, effectively doubling the available data size, does not compromise prediction capabilities. This is because the data collected with both systems (MOCAP and MAK) show irrelevant differences in estimated gait measurements, which makes the data interchangeable and integrable, allowing for the creation of high-performing machine learning models with strong predictive accuracies.

All findings derived from the analysis confirm that data from the MAK system enable the prediction of both normal and pathological gait profiles with an accuracy comparable to that of the MOCAP system despite the measurement differences highlighted by traditional validation metrics. This supports our initial hypothesis and answers the research question. Furthermore, the results emphasize the potential of machine learning approaches in supporting the validation of alternative movement analysis solutions and enhancing the understanding and interpretation of each gait profile. This makes machine learning a valuable tool for evaluating gait improvements or deterioration, particularly for monitoring and rehabilitation purposes.

5. Discussion

Gait analysis is a powerful and consolidated method for extracting information about walking patterns in both normal and pathological conditions. While MOCAP systems are considered the gold standard for instrumented gait analysis, their use is typically confined to clinical and research settings. As a result, several more practical and low-cost alternatives have been proposed in recent years to enable their widespread use in every day and unsupervised environments. However, despite their greater portability and reduced invasiveness, these alternatives generally exhibit lower accuracy than MOCAP systems. Analyzing the performance of these solutions in measuring gait features is therefore crucial before adopting them as tools for monitoring gait changes outside clinical contexts. Validation procedures, which involve comparing gait parameters from MOCAP systems and from new technologies, typically rely on statistical analysis and metrics. However, this approach may be influenced by intrinsic differences between the two systems, such as signal sources, data processing, non-simultaneous recording, biomechanical models, and parameter estimation algorithms. As a result, the performance of new technologies is often underestimated, even when differences in measurements could be insignificant for assessing overall gait patterns.

To the best of our knowledge, machine learning models, which are primarily used for classification and severity staging, have rarely been employed in the validation of new technologies to overcome the direct comparison of gait measurements. Therefore, this study aims to address this gap by thoroughly exploring the potential of integrating a machine learning approach into the validation process, demonstrating the equivalence of parameters estimated from MOCAP and MAK data despite their differences, and moving beyond traditional validation procedures that rely solely on statistical metrics.

To support our hypothesis, the first stage of the study involved using traditional statistical metrics to compare two datasets of unique gait profiles (UGPs) recorded by the MOCAP and MAK systems. Each dataset includes UGPs corresponding to both healthy and post-stroke individuals. Each UGP consists of spatiotemporal, asymmetry, and body

center of mass parameters that characterize the peculiarities of the walking pattern of each subject.

The analysis of medians and quartiles for both datasets revealed many similarities between gait measurements: although differences are observed in nearly all estimated parameters, only a few show significant discrepancies. MAE and RMSE indicate lower errors for all spatiotemporal and BCOM parameters. In contrast, asymmetry parameters exhibit maximum errors of approximately 12.1%. This behavior was expected, as asymmetry parameters are derived from spatiotemporal parameters and may propagate estimation errors, especially in non-simultaneous recordings.

Continuing with the analysis, the correlation values confirmed previous findings, revealing lower performance for asymmetry parameters, both between MOCAP and MAK data and between systems and participant groups. Spearman's correlation values between systems ($|\rho_0|$) exceed 0.75 for all spatiotemporal and BCOM parameters (Table 3), while correlations with participant groups ($|\rho_1|$) are slightly lower for both systems. In addition, ICC and CCC further validate the strong agreement and concordance between gait measurements from both systems. These validation results, based on traditional statistical metrics, align with findings from other studies comparing MOCAP and MAK systems, which report higher correlations than previous Kinect models [72,73]. Other studies have also documented strong correlations for spatiotemporal [74] and BCOM parameters [43,44]. However, exceptions have been noted for short temporal phases of gait cycles (such as foot off, double support, and swing time), particularly at higher speeds [34,75]. It is important to remember the challenges in comparing results across studies due to different protocols and target populations. Nevertheless, the findings of this study demonstrate that MAK-based systems can measure gait parameters with accuracy comparable to MOCAP systems despite differences in biomechanical models, data sources, processing methods, and parameter estimation algorithms.

In the second stage, a machine learning approach was integrated into the validation process to demonstrate that residual measurement differences do not impede the accurate assessment of normal and pathological gait profiles, reinforcing the findings from traditional statistical metrics. Various machine learning models were applied to the MOCAP dataset to identify the most effective model for gait profile assessments, achieving an accuracy of 98.7%. The analysis determined that the SVM with a linear kernel was the optimal model for MOCAP data, whether using all the UGP parameters or a selected subset. In both cases, only one post-stroke gait profile was misclassified (ID 64), with its parameters showing closer similarity to healthy control gait profiles, as illustrated in Figure 4. An SVM model with the same configuration was then applied to the MAK dataset (DB_MAK), achieving the same accuracy (98.7%) and misclassification rate (i.e., the same post-stroke gait profile). These findings confirm that residual measurement differences between the two systems are insignificant when assessing overall gait profiles. In addition, the analysis of posterior probabilities supports this conclusion, demonstrating a probability exceeding 95% of correctly assessing healthy control and post-stroke gait profiles for both systems (Table 7).

The final analysis demonstrated the interchangeability of the datasets, achieving accuracy exceeding 96%, and confirmed their integrability, enabling the effective doubling of the dataset size without compromising prediction performance (accuracy: 98.7%). These findings once again underscore the substantial agreement between the two systems in terms of overall predictive capability, enhancing the validity of the measurements and providing new and innovative insights into the assessment of normal and pathological gait profiles.

Despite the promising and encouraging findings, this study is not without limitations. The primary limitation is the relatively small size of the datasets, which could affect the generalizability of the results. Nevertheless, this study demonstrates that integrating a machine learning approach into the traditional validation process is highly effective for assessing overall normal and pathological walking patterns. Moreover, this methodology

has the potential to enable remote monitoring of gait changes and the timely detection of deviations from typical walking behaviors. Low-impact and easily deployable tools, such as camera-based solutions, could facilitate such applications in scenarios where traditional MOCAP systems are impractical. Furthermore, this approach supports the widespread detection of gait disorders, which can then be investigated in depth in clinical settings through diagnostic instrumented gait analysis using MOCAP systems to precisely quantify any detected abnormalities. Additionally, the use of machine learning posterior probabilities provides valuable insights into misclassified gait profiles, allowing a deeper understanding of individual parameters. This capability could also be a straightforward and synthetic metric for tracking gait improvements or deteriorations over time.

Secondly, we decided to include asymmetry parameters in the investigated UGP for the completeness of the gait analysis. However, in this study, these parameters were not particularly relevant for predicting normal and post-stroke gait profiles in both the MOCAP and MAK systems. This result could be due to the relatively lower number of post-stroke gait profiles (35 UGPs) compared to healthy control gait profiles (44 UGPs), where laterality in walking is less pronounced. Although some parameters (such as $ASYM_{STEPL}$ and $ASYM_{STEPT}$) show strong correlations between the systems, it will be necessary to expand the analysis of asymmetry metrics to a larger sample, including other pathological gait profiles. The lower reliability of other parameters suggests caution in the interpretation and application of asymmetry parameters derived from non-simultaneous acquisitions in clinical practice. Nevertheless, information about asymmetry could provide valuable insights for a more in-depth analysis of pathological gaits, which is why these parameters were considered in this study.

Moreover, this study explored only two configurations of parameters for training machine learning models. Specifically, the 12-parameter configuration was defined by selecting the most correlated parameters between the MOCAP and MAK systems. A more in-depth investigation of the most relevant configurations for machine learning models, using custom feature selection techniques and fine-tuning model parameters, could improve the results and help correctly resolve misclassified gait profiles. Finally, the machine learning models used in this study were trained on balanced datasets and binary classification problems, which simplified the training process. This decision allowed us to focus clearly on integrating ML models in the validation process rather than tackling more classical challenges that involve multiple subgroups or data stratification. However, exploring more complex scenarios (e.g., multiclass prediction or imbalanced data) would further enhance the relevance of the proposed approach. In the future, we intend to investigate more challenging case studies, such as including additional pathological gait profiles or clinical severity scales in the analysis, thus thoroughly exploring the potential and providing further insights into using machine learning models for validating motion analysis systems.

6. Conclusions

This study contributes to advancing the validation of innovative and non-invasive solutions based on MAK and other RGB-D sensors in comparison to MOCAP systems, which are considered the gold standard for medical applications. This study highlights the potential of integrating machine learning models into the validation process, moving beyond simple measurement comparisons, especially in assessing overall gait profiles. This methodological approach could provide clinicians with a highly practical, applicable, and interpretable tool for preventive and rehabilitative care.

The findings of this study support the initial hypothesis of enhancing traditional validation methods by using machine learning models to assess the significance or irrelevance of residual measurement errors arising from heterogeneous biomechanical models, signal sources, parameter estimation algorithms, and other potential intrinsic factors.

In conclusion, while this study highlights the potential and innovation of the proposed approach, the generalizability of the findings will be addressed and further improved in

future research. This will be achieved by adopting simultaneous data collection, expanding the sample size and profile diversity (e.g., including additional pathological gait profiles and severity scales), and applying advanced feature selection and fine-tuning techniques to consolidate and enhance the current results. These efforts will enable the full realization of the impact of Microsoft Azure Kinect in assessing both normal and pathological gait patterns.

Author Contributions: Conceptualization, C.F. and G.A.; methodology, C.F., G.A., S.C. and V.C.; software, C.F. and G.A.; validation, C.F., S.C., G.M. and V.C.; formal analysis, C.F., G.A., S.C., G.M. and V.C.; investigation, C.F., G.A., S.C. and V.C.; resources, C.F., G.A., S.C., G.M. and L.V.; data curation, C.F., S.C. and L.V.; writing—original draft preparation, C.F. and G.A.; writing—review and editing, S.C., G.M., L.V. and V.C.; visualization, C.F. and G.A.; supervision, C.F. and V.C.; project administration, C.F.; funding acquisition, C.F. All authors have read and agreed to the published version of the manuscript.

Funding: This study was partially supported by the project "ReHome—Soluzioni ICT per la teleriabilitazione di disabilità cognitive e motorie originate da patologie neurologiche", Grant POR F.E.S.R. 2014/2020—Piattaforma Tecnologica Salute e Benessere from Regione Piemonte (Italy), and by "ADVISOR—AI-Powered Vision-based solutions for healthcare", an internal project of CNR-IEIIT.

Institutional Review Board Statement: This study was conducted according to the guidelines of the Declaration of Helsinki and approved by the local Ethics Committee of "Istituto Auxologico Italiano" (protocol code 2020_02_18_01, approved on 28 February 2020).

Informed Consent Statement: All subjects gave their informed consent for inclusion before they participated in the study.

Data Availability Statement: The original data presented in the study are available in ZENODO at https://zenodo.org/records/14049199 (accessed on 27 November 2024).

Conflicts of Interest: The authors declare no conflicts of interest.

References

1. Pirker, W.; Katzenschlager, R. Gait disorders in adults and the elderly: A clinical guide. *Wien Klin. Wochenschr.* **2017**, *129*, 81–95. [CrossRef] [PubMed]
2. Mahlknecht, P.; Kiechl, S.; Bloem, B.R.; Willeit, J.; Scherfler, C.; Gasperi, A.; Rungger, G.; Poewe, W.; Seppi, K. Prevalence and burden of gait disorders in elderly men and women aged 60–97 years: A population-based study. *PLoS ONE* **2013**, *8*, e69627. [CrossRef] [PubMed]
3. Bonanno, M.; De Nunzio, A.M.; Quartarone, A.; Militi, A.; Petralito, F.; Calabrò, R.S. Gait Analysis in Neurorehabilitation: From Research to Clinical Practice. *Bioengineering* **2023**, *10*, 785. [CrossRef] [PubMed]
4. Das, R.; Paul, S.; Mourya, G.K.; Kumar, N.; Hussain, M. Recent Trends and Practices Toward Assessment and Rehabilitation of Neurodegenerative Disorders: Insights from Human Gait. *Front. Neurosci.* **2022**, *16*, 859298. [CrossRef]
5. Cruz-Jimenez, M. Normal Changes in Gait and Mobility Problems in the Elderly. *Phys. Med. Rehabil. Clin. N. Am.* **2017**, *28*, 713–725. [CrossRef]
6. Mirelman, A.; Bonato, P.; Camicioli, R.; Ellis, T.D.; Giladi, N.; Hamilton, J.L.; Hass, C.J.; Hausdorff, J.M.; Pelosin, E.; Almeida, Q.J. Gait impairments in Parkinson's disease. *Lancet Neurol.* **2019**, *18*, 697–708. [CrossRef]
7. Callegari, B.; Garcez, D.R.; Júnior, A.T.V.D.C.; Almeida, A.D.S.S.C.; Candeira, S.R.A.; do Nascimento, N.I.C.; de Castro, K.J.S.; de Lima, R.C.; Barroso, T.G.C.P.; Souza, G.D.S.; et al. Gait patterns in ischemic and hemorrhagic post-stroke patients with delayed access to physiotherapy. *Hong Kong Physiother. J.* **2021**, *41*, 77–87. [CrossRef]
8. Cimolin, V.; Galli, M. Summary measures for clinical gait analysis: A literature review. *Gait Posture* **2014**, *39*, 1005–1010. [CrossRef]
9. Wren, T.A.L.; Tucker, C.A.; Rethlefsen, S.A.; Gorton, G.E., 3rd; Õunpuu, S. Clinical efficacy of instrumented gait analysis: Systematic review 2020 update. *Gait Posture* **2020**, *80*, 274–279. [CrossRef]
10. Wren, T.A.; Gorton, G.E., 3rd; Ounpuu, S.; Tucker, C.A. Efficacy of clinical gait analysis: A systematic review. *Gait Posture* **2011**, *34*, 149–153. [CrossRef]
11. McGinley, J.L.; Baker, R.; Wolfe, R.; Morris, M.E. The reliability of three-dimensional kinematic gait measurements: A systematic review. *Gait Posture* **2009**, *29*, 360–369. [CrossRef] [PubMed]
12. Kainz, H.; Graham, D.; Edwards, J.; Walsh, H.P.J.; Maine, S.; Boyd, R.N.; Lloyd, D.G.; Modenese, L.; Carty, C.P. Reliability of four models for clinical gait analysis. *Gait Posture* **2017**, *54*, 325–331. [CrossRef] [PubMed]
13. Summan, R.; Pierce, S.G.; Macleod, C.N.; Dobie, G.; Gears, T.; Lester, W.; Pritchett, P.; Smyth, P. Spatial calibration of large volume photogrammetry based metrology systems. *Measurement* **2015**, *68*, 189–200. [CrossRef]

14. Patrizi, A.; Pennestrì, E.; Valentini, P.P. Comparison between low-cost marker-less and high-end marker-based motion capture systems for the computer-aided assessment of working ergonomics. *Ergonomics* **2016**, *59*, 155–162. [CrossRef]
15. Hulleck, A.A.; Menoth Mohan, D.; Abdallah, N.; El Rich, M.; Khalaf, K. Present and future of gait assessment in clinical practice: Towards the application of novel trends and technologies. *Front. Med. Technol.* **2022**, *4*, 901331. [CrossRef]
16. Salchow-Hömmen, C.; Skrobot, M.; Jochner, M.C.E.; Schauer, T.; Kühn, A.A.; Wenger, N. Review-Emerging Portable Technologies for Gait Analysis in Neurological Disorders. *Front. Hum. Neurosci.* **2022**, *16*, 768575. [CrossRef]
17. Mason, R.; Pearson, L.T.; Barry, G.; Young, F.; Lennon, O.; Godfrey, A.; Stuart, S. Wearables for Running Gait Analysis: A Systematic Review. *Sports Med.* **2023**, *53*, 241–268. [CrossRef]
18. Hutabarat, Y.; Owaki, D.; Hayashibe, M. Recent Advances in Quantitative Gait Analysis Using Wearable Sensors: A Review. *IEEE Sens. J.* **2021**, *21*, 26470–26487. [CrossRef]
19. Mobbs, R.J.; Perring, J.; Raj, S.M.; Maharaj, M.; Yoong, N.K.M.; Sy, L.W.; Fonseka, R.D.; Natarajan, P.; Choy, W.J. Gait metrics analysis utilizing single-point inertial measurement units: A systematic review. *Mhealth* **2022**, *8*, 9. [CrossRef]
20. Vun, D.S.Y.; Bowers, R.; McGarry, A. Vision-based motion capture for the gait analysis of neurodegenerative diseases: A review. *Gait Posture* **2024**, *112*, 95–107. [CrossRef]
21. Colyer, S.L.; Evans, M.; Cosker, D.P.; Salo, A.I.T. A Review of the Evolution of Vision-Based Motion Analysis and the Integration of Advanced Computer Vision Methods Towards Developing a Markerless System. *Sports Med. Open* **2018**, *4*, 24. [CrossRef] [PubMed]
22. Schlachetzki, J.C.M.; Barth, J.; Marxreiter, F.; Gossler, J.; Kohl, Z.; Reinfelder, S.; Gassner, H.; Aminian, K.; Eskofier, B.M.; Winkler, J.; et al. Wearable sensors objectively measure gait parameters in Parkinson's disease. *PLoS ONE* **2017**, *12*, e0183989. [CrossRef] [PubMed]
23. Sigcha, L.; Borzì, L.; Amato, F.; Rechichi, I.; Ramos-Romero, C.; Cárdenas, A.; Gascó, L.; Olmo, G. Deep learning and wearable sensors for the diagnosis and monitoring of Parkinson's disease: A systematic review. *Expert Syst. Appl.* **2023**, *229 (Part A)*, 120541. [CrossRef]
24. Peters, D.M.; O'Brien, E.S.; Kamrud, K.E.; Roberts, S.M.; Rooney, T.A.; Thibodeau, K.P.; Balakrishnan, S.; Gell, N.; Mohapatra, S. Utilization of wearable technology to assess gait and mobility post-stroke: A systematic review. *J. Neuroeng. Rehabil.* **2021**, *18*, 67. [CrossRef] [PubMed]
25. Boukhennoufa, I.; Zhai, X.; Utti, V.; Jackson, J.; McDonald-Maier, K.D. Wearable sensors and machine learning in post-stroke rehabilitation assessment: A systematic review. *Biomed. Signal Process Control.* **2022**, *71*, 103197. [CrossRef]
26. Sparaco, M.; Lavorgna, L.; Conforti, R.; Tedeschi, G.; Bonavita, S. The Role of Wearable Devices in Multiple Sclerosis. *Mult. Scler. Int.* **2018**, *2018*, 7627643. [CrossRef]
27. Shah, V.V.; Rodriguez-Labrada, R.; Horak, F.B.; McNames, J.; Casey, H.; Hansson Floyd, K.; El-Gohary, M.; Schmahmann, J.D.; Rosenthal, L.S.; Perlman, S.; et al. Gait Variability in Spinocerebellar Ataxia Assessed Using Wearable Inertial Sensors. *Mov. Disord.* **2021**, *36*, 2922–2931. [CrossRef]
28. Romijnders, R.; Warmerdam, E.; Hansen, C.; Welzel, J.; Schmidt, G.; Maetzler, W. Validation of IMU-based gait event detection during curved walking and turning in older adults and Parkinson's Disease patients. *J. Neuroeng. Rehabil.* **2021**, *18*, 28. [CrossRef]
29. García-Villamil, G.; Neira-Álvarez, M.; Huertas-Hoyas, E.; Ramón-Jiménez, A.; Rodríguez-Sánchez, C. A Pilot Study to Validate a Wearable Inertial Sensor for Gait Assessment in Older Adults with Falls. *Sensors* **2021**, *21*, 4334. [CrossRef]
30. Zhao, J.; Bunn, F.E.; Perron, J.M.; Shen, E.; Allison, R.S. Gait assessment using the Kinect RGB-D sensor. In Proceedings of the 37th Annual International Conference of the IEEE Engineering in Medicine and Biology Society (EMBC), Milan, Italy, 25–29 August 2015; pp. 6679–6683.
31. Ma, Y.; Mithraratne, K.; Wilson, N.C.; Wang, X.; Ma, Y.; Zhang, Y. The Validity and Reliability of a Kinect v2-Based Gait Analysis System for Children with Cerebral Palsy. *Sensors* **2019**, *19*, 1660. [CrossRef]
32. Summa, S.; Tartarisco, G.; Favetta, M.; Buzakis, A.; Romano, A.; Bernava, G.M.; Vasco, G.; Pioggia, G.; Petrarca, M.; Castelli, E.; et al. Spatio-temporal parameters of ataxia gait dataset obtained with the Kinect. *Data Brief* **2020**, *32*, 106307. [CrossRef] [PubMed]
33. Álvarez, I.; Latorre, J.; Aguilar, M.; Pastor, P.; Llorens, R. Validity and sensitivity of instrumented postural and gait assessment using low-cost devices in Parkinson's disease. *J. Neuroeng. Rehabil.* **2020**, *17*, 149. [CrossRef] [PubMed]
34. Vilas-Boas, M.C.; Rocha, A.P.; Choupina, H.M.P.; Cardoso, M.N.; Fernandes, J.M.; Coelho, T.; Cunha, J.P.S. Validation of a Single RGB-D Camera for Gait Assessment of Polyneuropathy Patients. *Sensors* **2019**, *19*, 4929. [CrossRef] [PubMed]
35. Dubois, A.; Bresciani, J.P. Validation of an ambient system for the measurement of gait parameters. *J. Biomech.* **2018**, *69*, 175–180. [CrossRef]
36. Bower, K.; Thilarajah, S.; Pua, Y.H.; Williams, G.; Tan, D.; Mentiplay, B.; Denehy, L.; Clark, R. Dynamic balance and instrumented gait variables are independent predictors of falls following stroke. *J. Neuroeng. Rehabil.* **2019**, *16*, 3. [CrossRef]
37. Latorre, J.; Llorens, R.; Colomer, C.; Alcaniz, M. Reliability and comparison of Kinect-based methods for estimating spatiotemporal gait parameters of healthy and post-stroke individuals. *J. Biomech.* **2018**, *72*, 268–273. [CrossRef]
38. Rocha, A.P.; Choupina, H.; Fernandes, J.M.; Rosas, M.J.; Vaz, R.; Silva Cunha, J.P. Kinect v2 based system for Parkinson's disease assessment. *Annu. Int. Conf. IEEE Eng. Med. Biol. Soc.* **2015**, *2015*, 1279–1282.
39. Vismara, L.; Ferraris, C.; Amprimo, G.; Pettiti, G.; Buffone, F.; Tarantino, A.G.; Mauro, A.; Priano, L. Exergames as a rehabilitation tool to enhance the upper limbs functionality and performance in chronic stroke survivors: A preliminary study. *Front. Neurol.* **2024**, *15*, 1347755. [CrossRef]

40. Amprimo, G.; Masi, G.; Priano, L.; Azzaro, C.; Galli, F.; Pettiti, G.; Mauro, A.; Ferraris, C. Assessment Tasks and Virtual Exergames for Remote Monitoring of Parkinson's Disease: An Integrated Approach Based on Azure Kinect. *Sensors* **2022**, *22*, 8173. [CrossRef]
41. Cao, Y.; Li, B.Z.; Li, Q.N.; Xie, J.D.; Cao, B.Z.; Yu, S.Y. Kinect-based gait analyses of patients with Parkinson's disease, patients with stroke with hemiplegia, and healthy adults. *CNS Neurosci. Ther.* **2017**, *23*, 447–449. [CrossRef]
42. Clark, R.A.; Vernon, S.; Mentiplay, B.F.; Millr, K.J.; McGinley, J.L.; Pua, Y.H.; Paterson, K.; Bower, K.J. Instrumenting gait assessment using the Kinect in people living with stroke: Reliability and association with balance tests. *J. Neuroeng. Rehabil.* **2015**, *12*, 15. [CrossRef] [PubMed]
43. Ferraris, C.; Cimolin, V.; Vismara, L.; Votta, V.; Amprimo, G.; Cremascoli, R.; Galli, M.; Nerino, R.; Mauro, A.; Priano, L. Monitoring of Gait Parameters in Post-Stroke Individuals: A Feasibility Study Using RGB-D Sensors. *Sensors* **2021**, *21*, 5945. [CrossRef] [PubMed]
44. Cimolin, V.; Vismara, L.; Ferraris, C.; Amprimo, G.; Pettiti, G.; Lopez, R.; Galli, M.; Cremascoli, R.; Sinagra, S.; Mauro, A.; et al. Computation of Gait Parameters in Post Stroke and Parkinson's Disease: A Comparative Study Using RGB-D Sensors and Optoelectronic Systems. *Sensors* **2022**, *22*, 824. [CrossRef] [PubMed]
45. Prasanth, H.; Caban, M.; Keller, U.; Courtine, G.; Ijspeert, A.; Vallery, H.; von Zitzewitz, J. Wearable Sensor-Based Real-Time Gait Detection: A Systematic Review. *Sensors* **2021**, *21*, 2727. [CrossRef]
46. Kobsar, D.; Charlton, J.M.; Tse, C.; Esculier, J.-F.; Graffos, A.; Krowchuk, N.M.; Thatcher, D.; Hunt, M.A. Validity and reliability of wearable inertial sensors in healthy adult walking: A systematic review and meta-analysis. *J. Neuroeng. Rehabil.* **2020**, *17*, 62.
47. Cerfoglio, S.; Ferraris, C.; Vismara, L.; Amprimo, G.; Priano, L.; Pettiti, G.; Galli, M.; Mauro, A.; Cimolin, V. Kinect-Based Assessment of Lower Limbs during Gait in Post-Stroke Hemiplegic Patients: A Narrative Review. *Sensors* **2022**, *22*, 4910. [CrossRef]
48. Jourdan, T.; Debs, N.; Frindel, C. The Contribution of Machine Learning in the Validation of Commercial Wearable Sensors for Gait Monitoring in Patients: A Systematic Review. *Sensors* **2021**, *21*, 4808. [CrossRef]
49. Jakob, V.; Küderle, A.; Kluge, F.; Klucken, J.; Eskofier, B.M.; Winkler, J.; Winterholler, M.; Gassner, H. Validation of a Sensor-Based Gait Analysis System with a Gold-Standard Motion Capture System in Patients with Parkinson's Disease. *Sensors* **2021**, *21*, 7680. [CrossRef]
50. Ippisch, R.; Jelusic, A.; Bertram, J.; Schniepp, R.; Wuehr, M. mVEGAS—Mobile smartphone-based spatiotemporal gait analysis in healthy and ataxic gait disorders. *Gait Posture* **2022**, *97*, 80–85.
51. Carroll, K.; Kennedy, R.A.; Koutoulas, V.; Bui, M.; Kraan, C.M. Validation of shoe-worn Gait Up Physilog®5 wearable inertial sensors in adolescents. *Gait Posture* **2022**, *91*, 19–25.
52. de Fontenay, B.P.; Roy, J.S.; Dubois, B.; Bouyer, L.; Esculier, J.F. Validating Commercial Wearable Sensors for Running Gait Parameters Estimation. *IEEE Sens. J.* **2020**, *20*, 7783–7791. [CrossRef]
53. Werner, C.; Awai Easthope, C.; Curt, A.; Demkó, L. Towards a Mobile Gait Analysis for Patients with a Spinal Cord Injury: A Robust Algorithm Validated for Slow Walking Speeds. *Sensors* **2021**, *21*, 7381. [CrossRef] [PubMed]
54. Desai, R.; Martelli, D.; Alomar, J.A.; Agrawal, S.; Quinn, L.; Bishop, L. Validity and reliability of inertial measurement units for gait assessment within a post stroke population. *Top Stroke Rehabil.* **2024**, *31*, 235–243. [CrossRef]
55. Strongman, C.; Cavallerio, F.; Timmis, M.A.; Morrison, A. A Scoping Review of the Validity and Reliability of Smartphone Accelerometers When Collecting Kinematic Gait Data. *Sensors* **2023**, *23*, 8615. [CrossRef]
56. Balta, D.; Figari, G.; Paolini, G.; Pantzar-Castilla, E.; Riad, J.; Della Croce, U.; Cereatti, A. A Model-Based Markerless Protocol for Clinical Gait Analysis Based on a Single RGB-Depth Camera: Concurrent Validation on Patients with Cerebral Palsy. *IEEE Access* **2023**, *11*, 144377–144393. [CrossRef]
57. Liang, S.; Zhang, Y.; Diao, Y.; Li, G.; Zhao, G. The reliability and validity of gait analysis system using 3D markerless pose estimation algorithms. *Front. Bioeng. Biotechnol.* **2022**, *10*, 857975. [CrossRef]
58. Summa, S.; Tartarisco, G.; Favetta, M.; Buzachis, A.; Romano, A.; Bernava, G.M.; Sancesario, A.; Vasco, G.; Pioggia, G.; Petrarca, M.; et al. Validation of low-cost system for gait assessment in children with ataxia. *Comput. Methods Programs Biomed.* **2020**, *196*, 105705. [CrossRef]
59. Arizpe-Gómez, P.; Harms, K.; Janitzky, K.; Witt, K.; Hein, A. Towards automated self-administered motor status assessment: Validation of a depth camera system for gait feature analysis. *Biomed. Signal Process. Control.* **2024**, *87*, 105352. [CrossRef]
60. Kusuda, K.; Matsubara, S.; Noguchi, D.; Kuwahara, M.; Hamasaki, H.; Miwa, T.; Maeda, T.; Nakanishi, T.; Ninomiya, S.; Honda, K. Concurrent Validity of Depth-Sensor-Based Quantification of Compensatory Movements during the Swing Phase of Gait in Healthy Individuals. *Biomechanics* **2024**, *4*, 411–427. [CrossRef]
61. Ferraris, C.; Ronga, I.; Pratola, R.; Coppo, G.; Bosso, T.; Falco, S.; Amprimo, G.; Pettiti, G.; Lo Priore, S.; Priano, L.; et al. Usability of the REHOME Solution for the Telerehabilitation in Neurological Diseases: Preliminary Results on Motor and Cognitive Platforms. *Sensors* **2022**, *22*, 9467. [CrossRef]
62. Ferraris, C.; Amprimo, G.; Masi, G.; Vismara, L.; Cremascoli, R.; Sinagra, S.; Pettiti, G.; Mauro, A.; Priano, L. Evaluation of Arm Swing Features and Asymmetry during Gait in Parkinson's Disease Using the Azure Kinect Sensor. *Sensors* **2022**, *22*, 6282. [CrossRef] [PubMed]
63. Davis, R.B.; Ounpuu, S.; Tyburski, D.; Gage, J.R. A gait analysis data collection and reduction technique. *Hum. Mov. Sci.* **1991**, *10*, 575–587. [CrossRef]

64. Kadaba, M.P.; Ramakrishnan, H.K.; Wootten, M.E. Measurement of lower extremity kinematics during level walking. *J. Orthop. Res.* **1990**, *8*, 383–392. [CrossRef] [PubMed]
65. Liu, Z. 3D Skeletal Tracking on Azure Kinect. 2019. Available online: https://www.microsoft.com/en-us/research/uploads/prod/2020/01/AKBTSDK.pdf (accessed on 18 October 2024).
66. Da Gama, A.E.F.; de Menezes Chaves, T.; Fallavollita, P.; Figueiredo, L.S.; Teichrieb, V. Rehabilitation motion recognition based on the international biomechanical standards. *Expert Syst. Appl.* **2019**, *116*, 396–409. [CrossRef]
67. Tsai, Z.-R.; Kuo, C.-C.; Wang, C.-J.; Tsai, J.J.P.; Chou, H.-H. Validation of Gait Measurements on Short-Distance Walkways Using Azure Kinect DK in Patients Receiving Chronic Hemodialysis. *J. Pers. Med.* **2023**, *13*, 1181. [CrossRef]
68. Błażkiewicz, M.; Wiszomirska, I.; Wit, A. Comparison of four methods of calculating the symmetry of spatial-temporal parameters of gait. *Acta Bioeng. Biomech.* **2014**, *16*, 29–35.
69. Boudarham, J.; Roche, N.; Pradon, D.; Bonnyaud, C.; Bensmail, D.; Zory, R. Variations in kinematics during clinical gait analysis in stroke patients. *PLoS ONE* **2013**, *8*, e66421. [CrossRef]
70. Beauchet, O.; Allali, G.; Sekhon, H.; Verghese, J.; Guilain, S.; Steinmetz, J.P.; Kressig, R.W.; Barden, J.M.; Szturm, T.; Launay, C.P.; et al. Guidelines for Assessment of Gait and Reference Values for Spatiotemporal Gait Parameters in Older Adults: The Biomathics and Canadian Gait Consortiums Initiative. *Front. Hum. Neurosci.* **2017**, *11*, 353. [CrossRef]
71. Steinwart, I. Consistency of support vector machines and other regularized kernel classifiers. *IEEE Trans. Inf. Theory* **2005**, *51*, 128–142. [CrossRef]
72. Kurillo, G.; Hemingway, E.; Cheng, M.L.; Cheng, L. Evaluating the Accuracy of the Azure Kinect and Kinect v2. *Sensors* **2022**, *22*, 2469. [CrossRef]
73. Tolgyessy, M.; Dekan, M.; Chovanec, L.; Hubinsky, P. Evaluation of the Azure Kinect and Its Comparison to Kinect V1 and Kinect V2. *Sensors* **2021**, *21*, 413. [CrossRef] [PubMed]
74. Guess, T.M.; Bliss, R.; Hall, J.B.; Kiselica, A.M. Comparison of Azure Kinect overground gait spatiotemporal parameters to marker based optical motion capture. *Gait Posture* **2022**, *96*, 130–136. [CrossRef] [PubMed]
75. Xu, X.; McGorry, R.W.; Chou, L.-S.; Lin, J.-H.; Chang, C.-C. Accuracy of the Microsoft Kinect for measuring gait parameters during treadmill walking. *Gait Posture* **2015**, *42*, 145–151. [CrossRef] [PubMed]